Three-Dimensional Structure of Murine Anti-*p*-azophenylarsonate Fab 36-71. 1. X-ray Crystallography, Site-Directed Mutagenesis, and Modeling of the Complex with Hapten[†,‡]

Roland K. Strong,*[,§] Robert Campbell,[‖] David R. Rose,[‖] Gregory A. Petsko,[⊥] Jacqueline Sharon,[#] and Michael N. Margolies[○]

Mail Stop 156-29, California Institute of Technology, Pasadena, California 91125, Division of Biological Sciences, National Research Council Canada, Building M-54, Ottawa, Ontario K1A 0R6, Canada, Rosenstiel Basic Medical Sciences Research Center, Brandeis University, Waltham, Massachusetts 02254-9110, Departments of Pathology and Biochemistry, Boston University School of Medicine, 80 East Concord Street, Room K707, Boston, Massachusetts 02118, and Department of Surgery, Massachusetts General Hospital and Harvard Medical School, Boston, Massachusetts 02114

Received August 29, 1990; Revised Manuscript Received December 26, 1990

ABSTRACT: The structure of the antigen-binding fragment (Fab) of an anti-*p*-azophenylarsonate monoclonal antibody, 36-71, bearing a major cross-reactive idiotype of A/J mice has been refined to an *R* factor of 24.8% at a resolution of 1.85 Å. The previously solved partial structure of this Fab at a resolution of 2.9 Å (Rose et al., 1990) was used as an initial model for refinement against the high-resolution data. The complex with hapten has been modeled by docking the small-molecule crystal structure of phenylarsonic acid into the structure of the native Fab on the basis of a low-resolution electron density map of the complex. In this model, residue Arg-96 in the light chain and residues Asn-35, Trp-47, and Ser-99 in the heavy chain contact the arsonate moiety of the hapten; an additional bond is found between the arsonate group and a tightly bound water molecule. The phenyl moiety of the hapten packs against two tyrosine side chains at positions 50 and 106 in the heavy chain. Residue Arg-96 in the light chain had been implicated as involved in hapten binding on the basis of previous experiments, and indeed, this residue appears to play a crucial role in this model. Experiments employing site-directed mutagenesis directly support this conclusion. The heavy-chain complementarity-determining regions have novel conformations not previously observed in immunoglobulins except for the recently solved anti-*p*-azophenylarsonate Fab R19.9 (Lascombe et al., 1989).

Monoclonal antibodies specific for the hapten *p*-azophenylarsonate (Ars)[1] are useful probes into the structural basis of antigen/antibody and anti-idiotype/idiotype interactions. When A/J-strain mice are immunized with this hapten conjugated to a keyhole limpet hemocyanin carrier, the majority of the antibodies produced in response are members of a cross-reactive idiotype family (CRI_a or Id^{CR}) (Kuettner et al., 1972; Marshak-Rothstein et al., 1981). The evidence to date indicates that all Id^{CR+} anti-Ars antibodies are the result, in the secondary immune response, of the combination of a single set of gene segments encoding immunoglobulin variable regions [V_H Id^{CR} (Siekevitz et al., 1982, 1983), $DFL_{16.1e}$ (Landolfi et al., 1986), J_H2 (Wysocki et al., 1986), and $V\kappa10$ and $J\kappa1$ (Sanz & Capra, 1987; Wysocki et al., 1987)]. Secondary immune response anti-Ars antibodies bearing Id^{CR} typically contain somatic mutations which on average result in antibodies with higher affinity for the hapten [reviewed in Manser et al. (1987a)]. The dominance of Id^{CR} was explained by a relatively high intrinsic affinity of the unique germline-encoded variable domain expressing Id^{CR} and the ability of that domain to sustain somatic mutations which enhance affinity (Manser et al., 1985). Alternative explanations of idiotype dominance involve the regulation of antibody production by interactions ("network") of idiotypes with anti-idiotypes (Jerne, 1974). The structural features of anti-Ars antibodies which account for hapten specificity and their idiotypic determinants have thus been the subject of intense scrutiny [reviewed in Manser et al. (1987a) and Rathbun et al. (1988)]. Recently, the crystal structure of an Id^{CR-} anti-Ars Fab, R19.9 [IgG2b (κ)], was reported at 2.8-Å resolution (Lascombe et al., 1989).

Among a family of anti-Ars Id^{CR+} hybridoma antibodies studied (Marshak-Rothstein et al., 1980; Margolies et al., 1981), antibody 36-71 [IgG1 (κ)], obtained in a secondary immune response, binds C^2-(*p*-azophenylarsono)-L-tyrosine (Ars-tyrosine) with a 200-fold greater affinity than does the germline-encoded antibody 36-65 (Rothstein & Gefter, 1983). Sequence analysis of 36-71 revealed a total of 19 amino acid differences with respect to antibody 36-65: 8 in V_H and 11 in V_L (Sharon et al., 1989; see Figure 1). The majority (17)

[†] This work was supported by the U.S. Public Health Service through NIH Grants CA 24432, HL 19259, and AI 23909. J.S. is a recipient of an ACS scholar award.

[‡] The coordinates for this structure have been deposited in the Brookhaven Protein Data Bank.

* To whom correspondence should be addressed.

[§] California Institute of Technology.

[‖] National Research Council Canada.

[⊥] Brandeis University.

[#] Boston University School of Medicine.

[○] Massachusetts General Hospital and Harvard Medical School.

[1] Abbreviations: CDR, complementarity-determining region; C_H1, first heavy-chain constant domain; C_L, light-chain constant domain; *F*, structure factor amplitude; Fab, antigen-binding fragment of an antibody consisting of V_H–C_H1 and V_L–C_L; H chain, heavy chain; *I*, intensity; Id^{CR+}, bearing the cross-reactive idiotype predominant among A/J anti-*p*-azophenylarsonate antibodies; Id^{CR-}, lacking the cross-reactive idiotype predominant among A/J anti-phenylarsonate antibodies; Ig, immunoglobulin; L chain, light chain; Ars, *p*-azophenylarsonate; Ars-tyrosine: C^2-(*p*-azophenylarsono)-L-tyrosine; rms, root mean square; σ, standard deviation; V_H, heavy-chain variable domain; V_L, light-chain variable domain.

0006-2960/91/0430-3739$02.50/0

```
        1                 10                  20                  30 CDR1             40
R19.9H  ( N O T   S E Q U E N C E D ) - - - - - - - - - - - - - - - - - - V - - - - - - - - - - - - - - -
36-65H  E V Q L Q Q S G A E L V R A G S S V K M S C K A S G Y T F T S Y G I N W V K Q R P G Q G L E W I G
36-71H  - - - - - - - - V - - - - - - - - - - - - - - - - - - - - - - N - - - - - - - - - - - - - - - - -

        50          CDR2  60                  70                  80                  90
R19.9H  - - - - - K - - L S - - - - - - - - - - - - - - R - - - - - - - - - - - - - - - - - - - - - - - -
36-65H  Y I N P G N G Y T K Y N E K F K G K T T L T V D K S S S T A Y M Q L R S L T S E D S A V Y F C A R
36-71H  - N - - - - - - I T - - - - - - - - - - - - - - - - - N - - - - - - - - - - - - - - - - - - - - -

         100    CDR3    a   b c d         110                 120
R19.9H  - F - · - - - E/D L A V - - - - S - - - - - - - - - - -
36-65H  S V Y Y G G S  ·  · · · Y Y F D Y W G Q G T T L T V S S
36-71H  - E - - - - -  ·  · · · - K - - - - - - - - - - - - - -


        1                 10                  20           CDR1 30                  40
R19.9L  - - - - - - - - - - - - - - - - - - - - - - - - ? - - - - - ? - - - - - - - - - - - - - - - - - -
36-65L  D I Q M T Q T T S S L S A S L G D R V T I S C R A S Q D I S N Y L N W Y Q Q K P D G T V K L L I Y
36-71L  - - - - - - I P - - - - - - - - - - - S - - - - - - - - - N - F - - - - - - - - - - S I - - - - -

        50 CDR2             60                  70                  80                  90 CDR3
R19.9L  - - - - - ? - - - - - - - - - - - - - - - - - - - - - - - - H - - - - - - - - - - - S - - - - - -
36-65L  Y T S R L E S G V P S R F S G S G S G T D Y S L T I S N L E Q E D I A T Y F C Q Q G N T L P R T F
36-71L  F - - - S Q - - - - - - - - - - - - - - - - - - - - - - - - - - - - - - - - - - - - - A - - - - -

          100
R19.9L  - - - - - - ? - ? -
36-65L  G G G T K L E I K R
36-71L  - - - - - - - - - -
```

FIGURE 1: Amino acid sequences of the variable domains of the H chain (top) and L chain (bottom) of 36-65 (Siekevitz et al., 1982; Wysocki et al., 1987; Parhami-Seren et al., 1989), 36–71 (Sharon et al., 1989), and R19.9 (Lascombe et al., 1989) are shown. The sequences are compared to that of the germline 36-65 antibody; *dashes* indicate sequence identity; *dots* denote gaps in the sequences introduced to maximize homology. The one-letter code for amino acids is employed (IUPAC–IUB); numbering is sequential relative to the 36-65 sequence; the insertion in R19.9 relative to 36-65 and 36-71 is numbered 105a–105d. Question marks in the R19.9 sequence indicate undetermined residues; a *slash* indicates an ambiguous residue assignment.

of these are due to somatic mutations; 2 are the result of D gene junctional differences. Experiments employing site-directed mutagenesis of the V_H region of 36-65 indicated that several of these mutations account for the enhanced affinity (Sharon, 1990). We previously published a preliminary model of the antigen binding fragment (Fab) of antibody 36-71 at 2.9-Å resolution (Rose et al., 1990). On the basis of this model, we report here the refined three-dimensional structure of the 36-71 Fab at 1.85-Å resolution. We also present a model of the complex between the Fab and hapten. The model is supported by previous results obtained by comparing sequences of anti-Ars Id^{CR+} antibodies with known binding properties and the results of experiments utilizing site-directed mutagenesis.

Materials and Methods

Data Collection. Data were collected from a single crystal of the 36-71 Fab grown as previously described (Rose et al, 1990) using a Hamlin-type area detector (Xuong et al., 1985) mounted on a Rigaku RU-200 rotating-anode X-ray generator. The UCSD data collection and reduction package (Howard et al., 1985) was employed to reduce the raw detector frames to structure factor amplitudes (F's). Reflections were measured out to 1.70-Å resolution; 79.5% of the theoretically obtainable data to a resolution of 1.85 Å were collected. The average signal-to-noise ratio [$I/\sigma(I)$] in the 2.14–2.07-Å shell is 2.0; the shell $I/\sigma(I)$ falls to a value of 1.29 in the 1.87–1.85-Å shell. The R_{obs}[2] = 6.64% including all measurements (calculated on intensities). Data were measured to an average redundancy of 4.1. The refined unit-cell parameters (space group $P2_1$) are a = 67.13 Å, b = 73.05 Å, c = 46.78 Å, β = 104.48°.

Refinement. The differences between F's calculated from the atomic model and the observed X-ray data were minimized through the use of two refinement methods: refinement by simulated annealing using the X-PLOR software package (Brünger et al., 1987), followed by least-squares refinement using the program PROLSQ (Hendrikson & Konnert, 1980). The refined, partial structure of this Fab to 2.9-Å resolution (Rose et al. 1990) was used as the initial set of coordinates. The initial R factor[3] calculated with this model and the area detector data was 44.3% on all F_{obs} to 1.85 Å, and did not appreciably decrease when the resolution range was narrowed; the area detector data were globally scaled to the 2.9-Å resolution diffractometer data used for the refinement of the initial structure at 2.9-Å resolution (Rose et al., 1990). X-PLOR was used to reduce this initial discrepancy between the model and the high-resolution data and was run in several steps: (1) hydrogens were generated for the initial structure; (2) an initial R factor was calculated, and weights for the diffraction "energy" terms were computed; (3) 160 cycles of Powell energy minimization were performed prior to the dynamics run; (4) the structure was artificially heated to 4000 K and then slowly cooled to room temperature while the dynamics simulation was run (step size = 25 K; Brünger et al., 1990); (5) 115 cycles of Powell minimization were run; (6) individual B factors (Dodson et al., 1979) were refined. All simulated annealing calculations were performed on all the data from 10- to 1.85-Å resolution. The R factor after the initial minimization stage was 34.0%; at the end of "slow-cooling", it had been reduced to 29.9%. After refinement of individual B factors, the R factor had fallen to 28.6%.

At this point, electron density maps were calculated (coefficients: $3F_{obs} - 2F_{calc}$; phases were calculated from the

[2] $R_{obs} \equiv \sum_{h,k,l}|\bar{I} - I_{obs}|/\sum_{h,k,l}\bar{I}$.

[3] R factor $\equiv \sum_{h,k,l}||F_{obs}| - |F_{calc}||/\sum_{h,k,l}|F_{obs}|$ (on all F_{obs}'s).

refined model) which contained clear and continuous density throughout the constant domains and the framework regions. Examination of this map also showed electron density, of variable quality, for all 21 residues in heavy (H) chain complementarity-determining region (CDR) 2 (positions 52–66) and HCDR3 (positions 101–106) which had not been placed in the preliminary 2.9-Å resolution model (Rose et al., 1990).[4] These 21 residues were then built into the model by using the program FRODO (Jones, 1978), although residues from 55 to 59 in HCDR2 were built as alanines due to the lower quality of the electron density map in this region. This model was then used as a starting point for PROLSQ refinement. The initial R factor for the complete structure after inclusion of the missing residues was 31.0%.

A total of 41 cycles of PROLSQ refinement were carried out. Initially, all data were included from 8.0- to 1.70-Å resolution, although the resolution range was gradually restricted to 6.0–1.85-Å resolution by the eighth cycle. Individual B factors were refined during each cycle. After 11 cycles, residues 55–59 were removed from the model due to their high B factors. After 10 more cycles (a total of 21), the structure was entirely rebuilt against electron density maps calculated with coefficients of the form $2F_{obs} - F_{calc}$. It was found that part of the three heavy-chain CDRs had been incorrectly placed: HCDR3 passed through density resulting from HCDR1, and HCDR1 had been built into density from HCDR2. The heavy-chain CDRs were corrected at this point, and at least partial side-chain density was present for all the residues except 59H, which was placed as an alanine. At this point, 163 crystallographic water molecules were built into the structure on the basis of $F_{obs} - F_{calc}$ electron density maps contoured at 2σ. Waters were only placed at locations where the proper number of hydrogen bonds could be made between appropriate donors and acceptors separated by 2.5–4.5 Å; none were placed within 6 Å of HCDR2 or HCDR3 due to the uncertainty in these sections.

Subsequently, 10 more cyles of refinement were carried out, followed by another round of rebuilding in which the chain traces of light (L)-chain CDR2 and LCDR3 were altered slightly. In addition, 19 water molecules were removed on the basis of high B factors (>45 Å^2), and 119 molecules were added to bring the total to 263 crystallographic water molecules, again on the basis of $F_{obs} - F_{calc}$ electron density maps contoured at 2σ. Rebuilding of the CDRs and any questionable region (such as the helical segments) was carried out aginst "delete maps" (Dodson, 1981) in which the residues of interest were deleted from the phasing model. All water molecules were excluded from the phasing model at this point for two reasons: to confirm the placement of the waters in the electron density map and to ensure that water molecules had not been placed into density better ascribed to protein. Inclusion of the crystallographic water molecules in the phasing model for these "delete maps" did not improve the observed electron density to the point of altering our interpretation of the placement of the atoms in the model at this stage. At this point, the electron density suggested that the solvent-exposed side chains of several residues might occupy two or more alternate conformations. In every case, the observed density implied that there was a single orientation which was of higher occupancy than any alternate conformation. The model of the Fab reflects these "best" conformations; alternate possibilities are not reflected in the final model or the final R factor.

[4] The numbering of amino acids in this report follows the sequential numbering of residues in the anti-*p*-azophenylarsonate antibody 36-65. There is an insertion of four residues in R19.9 relative to the other two sequences at position 105 in the heavy chain.

Table I: Refinement Statistics

constraint	rms	target σ
bond distances (Å)	0.022	0.030
angle distances (Å)	0.045	0.040
planar 1-4 distances (Å)	0.052	0.052
plane restraint (Å)	0.015	0.025
chiral centers (Å)	0.173	0.150
torsion angles: planar (0°, 180°)	3.3	5.0

3573 atoms
28713 F_{obs}'s 80.5% of the unique data from 6- to 1.85-Å resolution (all F's): R factor = 24.8% excluding 263 water molecules: R factor = 27.5%
22332 F_{obs}'s 62.2% of the unique data from 6- to 1.85-Å resolution ($F/\sigma F > 4$): R factor = 23.2%
9197 distances 444 (4.8%) bond distances deviate from ideality $>2\sigma$

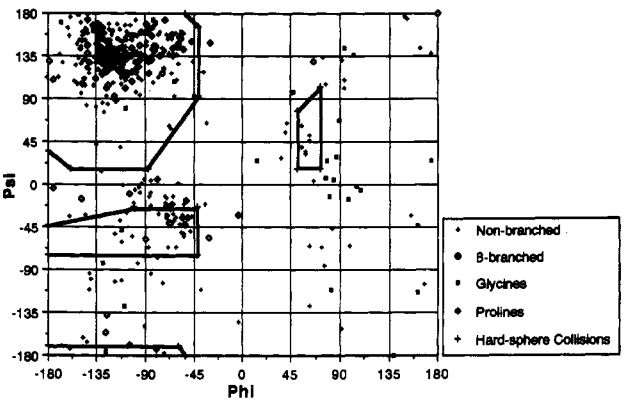

FIGURE 2: Main-chain torsion angles (ϕ/ψ; in degrees) of Fab 36-71 are displayed in this plot for each residue in the refined structure of Fab 36-71. The residues have been divided into classes based on the nature of the side chain. The sterically allowed regions of conformation space for the "outer limits" of the hard-sphere approximation are bordered by the *thick* lines (Ramachandran et al., 1963).

Finally, nine cycles of refinement were carried out until the R factor converged to 24.8%. The final geometric parameters for this structure are summarized in Table I. It was concluded, on the basis of a final round of inspection of the model against "delete" maps (with water molecules included in the phasing model), that the agreement between the model and the electron density could not be improved by further manual rebuilding. Since the model at this point was in good agreement with previously reported immunoglobulin structures in general, and Fab R19.9 specifically, and was in excellent agreement with the body of biochemical studies, sequence comparisons and site-directed mutagenesis experiments previously reported (see Results and Discussion), it was decided to terminate refinement. The estimated standard deviation in the atomic positions is 0.25 Å employing the method of Luzzati (1953). A plot of the main-chain torison angles (ϕ/ψ) for the final model is shown in Figure 2. The electron density is poorly defined for the side chains of the following residues: 7, 53, 154, 203, and 213 in the L chain; 40 and 139 in the H chain; and for the entirety of H-chain residues 41, 57, 66, 102, 120, 135, and 136. The calculations were performed on either a Convex C210 (X-PLOR) or a DEC Vaxstation 3200 (PROLSQ).

Generation and Analysis of Engineered Mutant Antibodies. The Arg-96 codon of V_L, a conserved residue in anti-Ars Id^{CR+} L chains (Jeske et al., 1984) including the three sequences presented in Figure 1, was converted to that for alanine by site-directed mutagenesis. The mutation was introduced into the rearranged 36-65 Vκ/Jκ gene (Wysocki et al., 1987) in M13MP19 (Norrander et al., 1983) by the two-primer method of oligonucleotide-directed mutagenesis (Zoller & Smith,

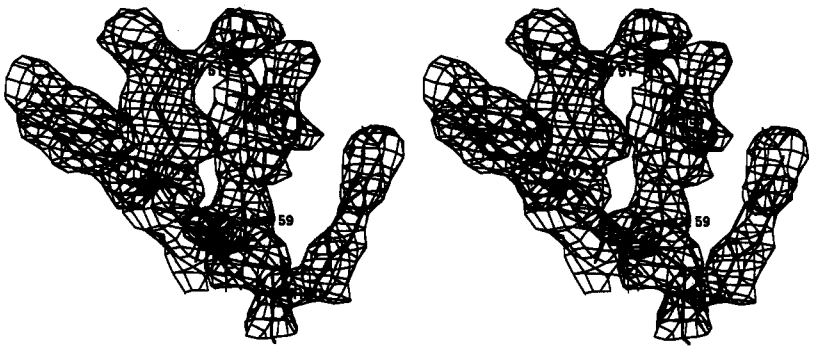

FIGURE 3: Representative electron density map of Fab 36-71 is displayed in this stereodiagram of residues 49H–51H and 57H–59H. The electron density map is a "delete map" contoured at 1σ (coefficients of the form $2F_{obs} - F_{calc}$) with phases calculated from the refined model with the displayed residues deleted.

1983) using the oligonucleotide 5′-G-CTT-CCT-GCG-ACG-TTC-G-3′ (substituted nucleotides are underlined). The mutation was verified by dideoxy nucleotide sequencing (Sanger et al., 1980) of the entire V_κ/J_κ gene. The mutant V_κ/J_κ gene, including 0.8 kilobase pair of upstream sequence and 1.5 kilobase pairs of downstream sequence, was transferred by enzymatic manipulations (Sambrook et al., 1989) out of M13MP19 into an expression vector containing both the H-chain and κ-chain enhancers upstream of a murine C_κ gene which includes transcriptional termination and polyadenylation signals (Sharon et al., 1984). The vector also contains the selectable marker neo which confers resistance to the antibiotic G418 (Southern & Berg, 1982). The resulting plasmid was transfected into the hybridoma cell line Sp2/0-Ag14, which secretes neither H nor L chains (Shulman et al., 1978), by spheroplast fusion as described (Sharon et al., 1986). Transfectomas were recovered in selective medium containing 1 mg/mL G418 (Gibco). The presence of κ chains in cell lysates (Sharon et al., 1986) was detected by immunoblot analysis (Towbin et al., 1979) using a rabbit anti-mouse κ antiserum and alkaline phosphatase conjugated anti-rabbit IgG and substrate obtained from Promega Biotec (ProtoBlot system). A transfectoma producing the κ chain was chosen for further analysis.

Vectors containing the Eco gpt gene which confers resistance to mycophenolic acid and γ2b H-chain genes encoding 36-65 or 36-71 V_H regions (Sharon 1990) were separately transfected into the κ chain producing cell line; transfectomas were recovered in double-selective medium containing G418 and mycophenolic acid [HMX medium (Mulligan & Berg, 1980)]. Analysis of transfectomas for IgG secretion was performed as previously decribed (Sharon et al., 1989). Mutant antibodies were purified from 1 L of culture supernatants on protein A–Sepharose (Pharmacia/LKB) according to the manufacturer's instructions. Affinities of mutant and wild-type antibodies for Ars-tyrosine were determined by fluorescence quenching at 23–25 °C as previously described (Rothstein & Gefter, 1983) using a Perkin-Elmer LS-3 fluorescence spectrophotometer and curve-fitting software written by J. Sharon and A. Sharon (Massachusetts Institute of Technology). Two binding sites per molecule were assumed for all antibodies.

RESULTS

The Structure of the Fab of the Anti-Ars Antibody 36-71 Was Refined against Data to 1.85-Å Resolution to an R Factor of 24.8%. The electron density maps are clear and unambiguous (see Figure 3 for a representative section of density), and are continuous except for a few sections where the refined individual *B* factors are quite high (see Figure 4). *B* factors are a measure of positional uncertainty, usually

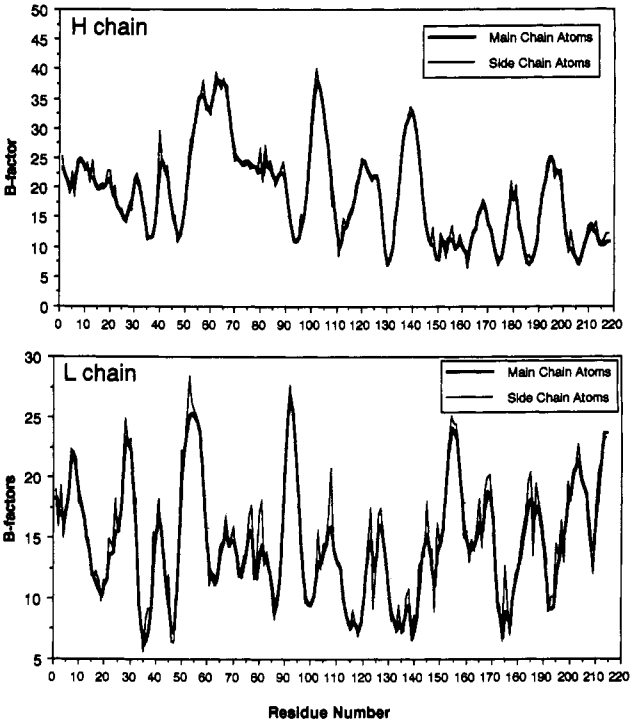

FIGURE 4: Plots for Fab 36-71 display the *B* factors (units of Å^2) for the H-chain residues (top) and the L-chain residues (bottom) calculated during the refinement of Fab 36-71. Averages for both the main-chain atoms and the side-chain atoms are shown.

associated with thermal motion (Dodson et al., 1979). The crystallographic water molecules account for 7.4% of the atoms in the final model, and lower the final *R* factor by 2.7% when present (see Table I).

The main differences between this structure and the previously reported 2.9-Å resolution structure (Rose et al., 1990) lie in the CDRs; our current structure is complete and has corrected several small errors in the chain trace of the LCDRs and HCDR1. The hypothesis based upon the 2.9-Å resolution data that the poor quality of the electron density maps in the region of HCDR2 and HCDR3 might be due to high thermal mobility as a result of a high degree of solvent exposure was confirmed by our current analysis [see Figure 4 and Strong et al. (1991)].[5]

The Domain Structure of 36-71 Is Consistent with All Other Fab Crystal Structures. The Cα backbone, including the tightly bound water molecules placed in our model, is shown in Figure 5, and is consistent with previously reported Fab structures [reviewed in Colman (1988), Fujinaga and

[5] See following paper (Strong et al., 1991) for further discussion.

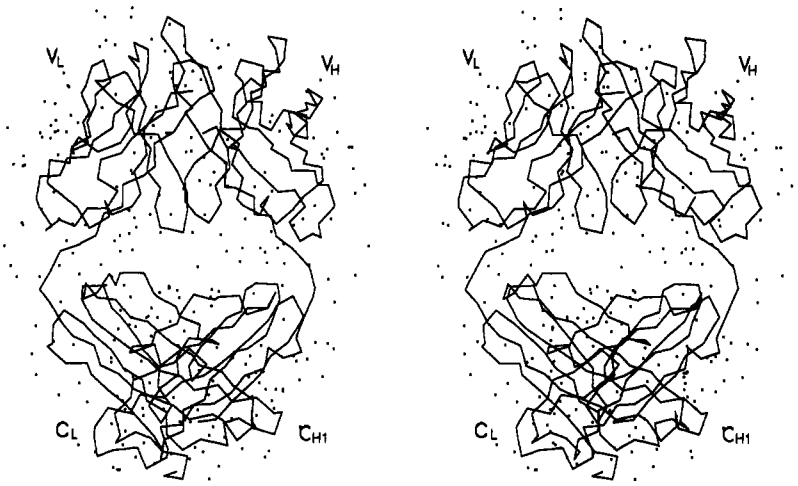

FIGURE 5: Stereodiagram shows the Cα backbone of Fab 36-71 after refinement. Included are all crystallographic water molecules placed during refinement. Crystal contacts are almost exclusively H chain to L chain/L chain to H chain. The variable domains are at the top of the figure, and the L chain is on the left hand side.

Read (1987), Cygler et al. (1987), Davies and Metzger (1983), and Amzel and Poljak (1979)]. The "elbow" angle of the molecule (the angle between the pseudodyad axes relating the variable domains and the constant domains of the two chains) is 179°, close to values for this class of molecules, but the highest (most linear) reported to date. The rotation–translation operations which superimpose the backbone of C_L onto C_H1 are 168° and 1.2 Å; for V_L onto V_H, 177° and 0.49 Å. These values are comparable to the corresponding parameters for the R19.9 Fab and have not changed significantly from the values of the Fab 36-71 2.9-Å resolution model (Rose et al., 1990), except for the "elbow" angle which was 164° for the 2.9-Å model. These quantities were calculated by comparing the positions of 43 α-carbon atoms in each of the constant domains and 66 α-carbons in each of the variable domains using the program COMPARE (Hendrickson, 1979). These Cα's were selected as conforming to the pseudodyads within the molecule better than the remaining Cα's on the basis of a visual inspection of the backbone structure of the refined model for 36-71.

Two short α-helical segments are present in C_L: residues 121–128L (two turns) and 184–187L (one turn). The pseudodyad-related segments in C_H1 are either only loosely helical in nature or involved in a highly mobile, exposed loop, represented by lower quality density (see the region around residue 139H in Figure 4). A short α-helical segment was found in Fab NEW (190–195H) and two segments of distorted α- or π-helices at 78–82H and 86–90H (Poljak et al., 1974). The 190–195H α-helix in Fab NEW is close to the corresponding location of the distorted helical segment in the H chain of Fab 36-71 (residues 194–198).

The Variable/Constant Domain Interface Is Dominated by Tightly Bound Water Molecules. The region between the variable domains and the constant domains consists of a large cavity (roughly 8–10-Å wide at the greatest breadth) which tapers toward the two "elbow" regions (approximately 104–110L and 110–116H). Examination of the distribution of crystallographic water molecules (see Figure 5) shows that a significant portion of the contacts between variable and constant domain pairs is through these waters just within the "elbows". The center third of the cavity is devoid of tightly bound waters, with no significant contacts across the interface.

The Conformation of HCDR2 Is Unique in Fab 36-71. The L-chain CDRs of 36-71 are similar in conformation to the LCDRs of Fabs or L-chain dimers which contain κ L chains for which coordinates are available [McPC603 (Segal et al., 1974), REI (Epp et al., 1976), J539 (Suh et al., 1986), and HyHEL-5 (Sheriff et al., 1987)][6] except in certain details. Residue Ile-29 in LCDR1, which is Val, Ile, or Leu in J539, REI, and McPC603, respectively, is similarly "buried" in 36-71. LCDR1 of 36-71 has an essentially identical conformation with LCDR1 in the crystal structure of the Fab of the anti-lysozyme antibody HyHEL10 (Padlan et al., 1989). LCDR2 has roughly the same conformation in 36-71 as in the other κ L chain containing molecules, except that residue 51 (Thr) is buried in 36-71, while the homologous residues are exposed to solvent in the other structures. LCDR3 in 36-71 is comparable in structure to LCDR3 in REI and McPC603. These results are not inconsistent with the reported observations of Chothia and Lesk (1987) and Chothia and co-workers (Chothia et al., 1989) that LCDR conformations are homologous between several different immunoglobulins. The heavy-chain CDRs, however, deviate in structure significantly from previously reported Fab structures. The path of the main chain of HCDR2 courses over HCDR1, makes a hairpin turn, passes over itself, goes through a distorted helical turn, and reenters the domain (see Figure 6). Both of the turns in HCDR2 are somewhat disordered as indicated by the elevated *B* factors displayed by these residues (see residues 55–56H and 62–68 H in Figure 4) and the "choppier" nature of the electron density maps in the regions corresponding to these residues. While following this path, HCDR2 blocks much of HCDR1 from solvent and lays down two short strands of distorted antiparallel β-sheet. The more solvent-exposed β-strand of HCDR2 corresponds to the "dip" in the *B*-factor plot at residues 57–61H; the disordered turns in HCDR2 account for the *B* factor "peaks" on both sides of residues 57–61H. HCDR3 has the conformation of a long hairpin loop, with residues 101–103H highly exposed to solvent. This conformation is similar to that observed in HCDR3 of McPC603, except that Tyr-106H points in the opposite direction in 36-71 to interact with hapten in the modeled complex (see below; the homologous residue in McPC603 packs against a phenylalanine residue at position 49L). The Cα's of the residues at the base of the hairpin turn (99H and 108H; these residues bracket the D gene encoded residues) are separated by only 4.0 Å, indicating the tightness of this loop.

The Complex of Fab 36-71 with Hapten at High Resolution Has Been Modeled on the Basis of Low-Resolution Data

[6] Structural comparisons to R19.9 are discussed in the following paper (Strong et al., 1991).

FIGURE 6: Stereo drawing shows the Cα backbone of the variable domains (V_L on the left, V_H on the right). The CDRs are indicated by heavy lines and labeled, and the modeled ligand, phenylarsonate, is included. For clarity, the labeling of the CDRs has been shortened from HCDR1, LCDR1, etc. to H1, L1, etc.

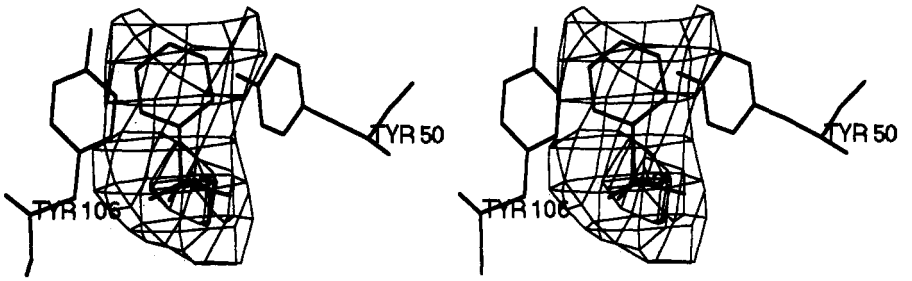

FIGURE 7: Low-resolution electron density map used to localize the hapten is shown in stereo in this figure. It is calculated from coefficients of the form $F_{derivative} - F_{native}$ for a heavy-atom derivative which included arsanilic acid; phases were calculated from the 1.85-Å resolution model. It is contoured at 2.2σ and 3.6σ, and includes data to 4.5-Å resolution. The aromatic residues which pack against the aryl moiety of the hapten are also shown; the arsenic atom of the hapten has also been labeled.

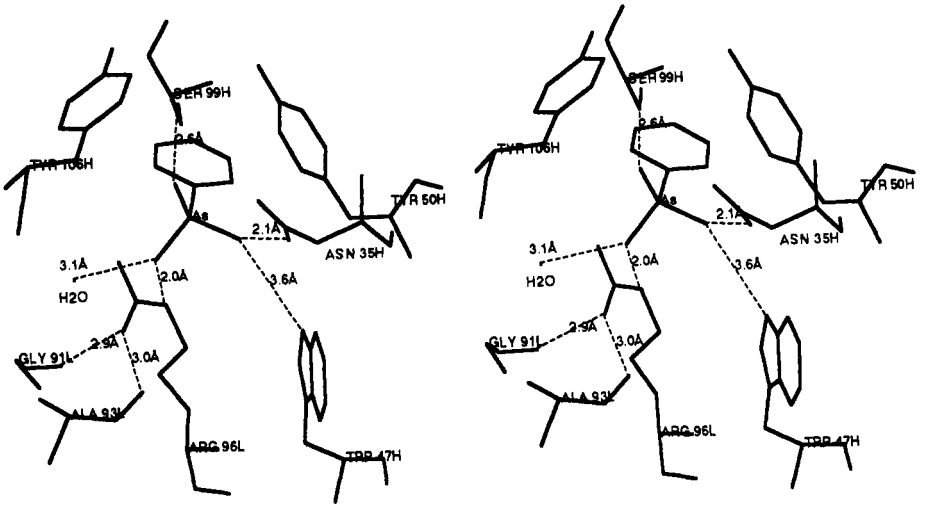

FIGURE 8: Coordination of the hapten in the model of the complex between Fab 36-71 and phenylarsonate is shown in stereo in this figure. Included are any relevant hydrogen bonds and distances. The structure of the hapten is that of the reported crystal structure of phenylarsonate (Shimada, 1960) except to place it in the refined structure of the native Fab which has not been altered to improve the fit with hapten. The arsenic atom of the hapten has also been labeled.

Measured from the Complex. Difference Fourier syntheses, using coefficients of the form $F_{derivative} - F_{native}$ from one of the heavy-atom derivatives used in the initial phasing of the structure (Rose et al., 1990) and refined phases from the 1.85-Å resolution model, provide information localizing the binding site of phenylarsonate. This derivative was formed with ethylmercury phosphate and arsanilic acid. In the refined structure reported here, strong density not accounted for by the mercury compound appears in one location (see Figure 7). On the basis of this low-resolution information localizing the arsenic atom, we have been able to fit the small-molecule structure of phenylarsonate (Shimada, 1960) into the combining site of Fab 36-71 to model the complex between the native Fab and hapten (see Figure 8) by rotating the phenylarsonate structure rigidly around the presumed arsenic atom position to optimize hydrogen and van der Waals bonds to the Fab while minimizing unfavorable steric interactions. Hydrogen bonds to the arsonate moiety are provided by the side chains of residues in the CDRs (Arg-96L, Asn-35H, and Ser-99H), a tightly bound water molecule (H_2O 799), and potentially a framework residue (Trp-47H). In addition, the aryl moiety packs against the side chains of two aromatic resides in HCDR2 and HCDR3 (Tyr-50H and Tyr-106H). Interestingly, Arg-96L does not appear to interact with the arsonate group through the terminal nitrogens, but rather through its ε-N atom; one terminal nitrogen makes hydrogen bonds to two main-chain carbonyl groups (Gly-91L and Ala-93L), which position the ε-N atom for optimal binding. This binding site lies at the bottom of a conical "pit" formed by LCDR3, HCDR2, and HCDR3. The opening of this

Table II: Binding Constants of Wild-Type and Mutant Antibodies for Ars-Tyrosine[a]

protein tested	$K_{a'} \times 10^5$ M^{-1} (relative affinity) with 36-65 L chain	with 36-71 L chain
wild-type H chain		
36-65	1.64 (1.0)	2.36 (1.0)
36-71	270 (165)	313 (133)
36-65 mutant H chain		
Thr-58/Lys-59/Tyr-107 → Ile/Thr/Lys	395 (241)	489 (207)
Thr-58/Lys-59/Val-100/Tyr-107 → Ile/Thr/Glu/Lys	40 (24)	244 (103)
36-65 mutant L chain		
Arg-96 → Ala	none detected (0)	none detected (0)

protein tested	$K_{a'} \times 10^5$ M^{-1} (relative affinity)
hybridoma protein	
36-65	1.79 (1.0)
36-71	372 (227)

[a] Binding constants were determined by fluorescence quenching with Ars-tyrosine at 23–25 °C (Sharon, 1990). The results for the 36-65 mutant L chain are reported herein.

conical "pit" is not perpendicular to the V_H/V_L pseudodyad; rather, it is canted forward (toward LCDR3) such that HCDR2 and HCDR3 form a back "wall" against which the aryl moiety of the hapten rests. Our model for the complex places the arsenic atom of the hapten very nearly on the pseudodyad axis relating V_H to V_L. While some rearrangement of the liganding residues almost certainly occurs in the actual complex relative to the native structure of the Fab, the fit of the hapten in our structure is excellent. No information on such structural rearrangements is available from the derivative difference Fourier synthesis due to the low resolution (4.5 Å) of this synthesis.

The Loss of Ars-Tyrosine Affinity Observed in the Arg-96L to Ala Mutant Is Consistent with the Model of the Coordination of the Hapten in the Complex. To directly verify that Arg-96L contacts the hapten, as previously proposed by using evidence from sequence comparisons by Jeske and co-workers (Jeske et al., 1984), we produced two mutant antibodies in which position 96 of V_L was converted to alanine by site-directed mutagenesis. One of the mutant antibodies is in the background of the germline antibody 36-65 H and L chains, while the other is in the background of the 36-71 H chain and the 36-65 L chain (see Figure 1). [We have previously shown (Sharon, 1990) that a hybrid antibody consisting of the 36-71 H chain and the 36-65 L chain has a comparable affinity for Ars-tyrosine to 36-71 (see also Table II).] Analysis of [^{35}S]methionine biosynthetically labeled secreted proteins for binding to Ars–bovine serum albumin–Sepharose by electrophoresis of bound proteins (Sharon et al., 1986) in SDS–polyacrylamide gels (Laemmli, 1970) showed that both mutant antibodies produced here do not bind antigen. The mutant antibodies were purified on protein-A Sepharose and quantitatively analyzed for Ars-tyrosine binding by fluorescence quenching. As shown in Table II, no detectable binding was observed with either of the two Ala-96L mutant antibodies, even though the method can detect binding constants in the 10^4 M^{-1} range. From these experiments, we conclude that the Arg-96L to Ala mutation abolishes specific binding of the antibodies to the Ars hapten.

Discussion

Differences Exist between the 2.9-Å Structure and the Current 1.85-Å Model. All residues in HCDR2 and HCDR3 not defined at 2.9-Å resolution are present in the current model. At 1.85-Å resolution, the chain trace is slightly different in the regions of the CDRs, as is the conformation of the residues in the combining site. In general, the residues in the hapten-binding site have a slightly more "open" conformation than that defined in the preliminary model. While we had tentatively identified the correct binding site in the 2.9-Å structure, Ser-99H [a residue identified as a requirement for Ars binding (Sharon et al., 1986)] did not appear to be directly involved in hapten binding. This residue clearly provides an important ligand to the hapten in the current model. In addition, HCDR3, which forms part of the "back wall" of the combining site, isolates the binding site from several residues. Most important of these is Lys-107H which had been identified (Rose et al., 1990) as potentially involved with interactions to Ars-tyrosine in the 2.9-Å model, a compound used in many of the binding assays (Kresina et al., 1982; Rothstein & Gefter, 1983). The current model would indicate that the tyrosine moiety of Ars-tyrosine would continue out the top of the molecule, approximately along the pseudodyad of the variable domains, and not lay back over the top surface of the molecule, as the earlier model had suggested. There is room in the current model of Fab 36-71 to accommodate Ars-tyrosine in the binding site with an attached, conjugated carrier-protein on the antibody surface.

The Individual B Factors Calculated during the Refinement Are Strongly Correlated with Physical Aspects of the Structure. In Figure 4, the "peak–valley–peak" nature of the *B*-factor plots follows precisely the "turn–sheet–turn" nature of immunoglobulin domains. The CDRs (HCDR1, 31–35; HCDR2, 50–66; HCDR3, 99–110; LCDR1, 24–34; LCDR2, 50–56; LCDR3, 89–97) generally account for the highest peaks. The "elbow" regions likewise have relatively high *B* factors. The helical segments (residues 121–128L and 184–187L) display a characteristic split-peak pattern, which is weakly echoed in the pseudo-dyad-related region at 194–198H. The partially disordered "loop" in C_H corresponding to the α-helical segment from 121 to 128L in C_L appears as a prominent peak in the plot centered around 193H. In general, the *B* factors for the L chain are lower than for the H chain, consistent with the observation that the electron density for the L chain is clearer and easier to interpret. The overall values for the refined *B* factors are consistent with those observed for other protein structures (Hartmann et al., 1982). *B* factors in the range of 12–15Å^2 correspond to mean-square atomic displacements of 0.15–0.18 Å (Ringe & Petsko, 1985).

Many of the Putative Contact Residues in the Modeled Complex with Hapten Are Highly Conserved. On the basis of chain recombination experiments and sequence analysis, it was proposed that the conserved V_κ–J_κ junctional residue Arg-96L was required for Ars binding (Jeske et al., 1984). The mutagenesis experiments reported here (see Table II) directly support this contention and are consistent with the crystal structure. We tabulated the available amino acid and/or nucleotide sequences of anti-Ars antibodies which utilize the V_H Id^{CR} gene and have been shown to bind Ars (Estess et al., 1980; Marshak-Rothstein et al., 1980; Margolies et al., 1981; Siegelman et al., 1981; Siekevitz et al., 1982; Alkan et al., 1983; Ball et al., 1983; Slaughter & Capra, 1983; Gridley et al., 1985; Slaughter et al., 1985; Wysocki et al., 1985, 1986, 1987, 1990; Haba et al., 1986; Fish & Manser, 1987; Manser et al., 1987b; Meek et al., 1987; Rathbun et al., 1988; Sharon et al., 1989; Fish et al., 1989; Lascombe et al., 1989; Parhami-Seren et al., 1989, 1990). Among 48 such antibodies which also utilize the V_κ10 germline gene associated

with the predominant idiotype, for which the sequence at 96L is known, all contain arginine (see Figure 1).

Among the H-chain residues which contact hapten in the modeled complex of Fab 36-71, Asn-35H in CDR1 is conserved (unmutated) in all of the 81 Ars-binding antibodies utilizing V_H Id^{CR} for which sequence data are available at that position. The framework residue Trp-47H is conserved in 43 of 44 available sequences. (The exception may be an error in Edman degradation of an intact H chain.) Tyrosine is found at position 50H in CDR2 in 80 of 82 antibodies sequenced at that position; the exceptions include a highly mutated antibody (hVH 65–110; Manser et al., 1987b) with reduced affinity relative to the germline-encoded antibody 36-65 and an antibody (9ABA2′-3; Fish et al., 1989) which utilizes noncanonical D and V_κ genes.[7] Positions 35H, 47H, and 50H are encoded by the V_H Id^{CR} gene. However, the Ser-99H residue is not encoded in the germline V_H or D gene sequences (Wysocki et al., 1986; Milner et al., 1986) yet is highly conserved. Although a mutant with Thr-99H binds Ars equally well, suggesting that the hydroxyl is necessary and sufficient for binding (Sharon et al., 1986), this residue has never been observed at that position, perhaps related to the mechanism for generation of this junctional residue. Ser-99H is essentially inaccessible to solvent; the additional methyl group of a threonine residue could, however, be accommodated at the very bottom of the combining site "pit". Among 83 Ars-binding antibodies utilizing V_H Id^{CR} for which the residue at position 99 was determined, 75 contain serine at this position. In each of the eight exceptions (Fish & Manser, 1987; Wysocki et al., 1986), one or more of the following major structural differences are also present: use of a noncanonical $V\kappa$ sequence (seven of eight sequences), use of a noncanonical D gene segment (one example), or use of a noncanonical J_H gene segment (six sequences). Thus, in all known instances in which the canonical set of gene segments is utilized in Ars-binding hybridoma proteins, serine is conserved at position 99H.

The Tyr residue at position 106H is encoded by the D gene (Landolfi et al., 1986) and is conserved in 63 of 64 Ars-binding antibodies sequenced at that position which utilize the canonical gene segment combination. The one exception (hVH 65–107; Manser et al., 1987b) has Phe at this position as well as multiple somatic mutations at other positions, the sum of which results in reduced Ars affinity. Seven other Ars-binding antibodies which utilize V_H Id^{CR} contain substitutions at position 106H, but all of these utilize one or more noncanonical gene segments.

Thus, the remarkable degree of conservation among the six residues Arg-96L, Asn-35H, Trp-47H, Tyr-50H, and Tyr-106H lends further support to the proposed modeled complex of Fab 36-71 with hapten and suggests that the combining sites of other anti-Ars antibodies bearing the predominant idiotype may be similar in structure.

With respect to residues coordinating with Arg-96L that could potentially affect Ars binding, Gly is present at position 91L among 49 Ars-binding antibodies which utilize the V_H Id^{CR} and $V\kappa$ 10 genes for which the sequence is known. The single exception (Ser) is in a highly mutated antibody (hVH 65–110; Manser et al., 1987b) with reduced Ars affinity. However, the germline Thr-93L present in 42 of 50 available sequences can be mutated to Ser, Met, or Ala in antibodies utilizing the canonical gene segment combination which retain Ars binding.

[7] In this report, "canonical" refers to the specific set of gene segments found in murine anti-Ars antibodies expressing Id^{CR}.

The Three-Dimensional Structures of the CDRs Are Not Independent of the Structure of the Rest of the Molecule. It has been suggested that most of the CDRs of Igs have one of a small, discrete set of main-chain conformations, or canonical structures, determined by various conserved residues within these regions (Chothia & Lesk, 1987; Chothia et al., 1989). The conformations of LCDR1 and LCDR3, though different in detail, do not contradict this hypothesis. However, HCDR1 and HCDR2 show a high degree of structural interdependence (see Figure 7). Clearly, the structure of HCDR2 depends to a great extent on the underlying surface, which partially consists of HCDR1.

Structural interdependencies on a lesser scale become apparent when comparing the three-dimensional structures of 36-71 and the anti-Ars hybridoma antibody R19.9 (Lascombe et al., 1989). Single-site substitutions in one CDR can affect the conformation of another CDR. For example, the mutation at position 32L of Tyr to Phe in 36-71 affects the conformation of HCDR3. Since the sequence of R19.9 is identical with the germline at many places where substitutions have occurred in 36-71 relative to 36-65, the structure of R19.9 can be used as a "model" for the structure of 36-65.[5] The interdependence of different CDRs can then be experimentally observed by comparing the binding constants of two H-chain-engineered mutants of 36-65 (Sharon, 1990; see Table II). The mutants containing multiple changes at positions 58H, 59H, and 107H and at positions 58H, 59H, 100H, and 107H show the deleterious effect of a glutamic acid at position 100H. This residue is in a cleft behind the binding site between HCDR3 and HCDR1. The residue at this position is potentially capable of affecting the packing of the side chain of Tyr-50H, one of the residues contacting the hapten. However, the magnitude of the effect of the substitution at 100H is 2-fold less when the mutant H chain is reconstituted with the 36-71 L chain, and is 10-fold lower when reconstituted with the 36-65 L chain (Table II). Clearly, the identity of the L chain modulates the effect of this position on hapten affinity in these mutant antibodies. The most likely explanation based on the crystal structure is that the substitutions at positions 32L and 50L affect the structure of the binding site by altering the conformation of HCDR3.

Furthermore, mutations in nonconserved residues within a CDR can have striking effects on the main-chain structure of the CDR; for example, note the changes in the structure of LCDR2 between 36-71 and R19.9.[6] At least in 36-71, it is important to view the conformations of each CDR in context with the remainder of the molecule.

The three-dimensional structure of the anti-Ars Fab 36-71 described in this report is consistent with and explains reported observations of hapten-binding affinities of anti-Ars hybridomas resulting from the somatic mutation process and gene junctional variation and of anti-Ars antibodies produced by mutagenesis. In the following paper (Strong et al., 1991), the structure of 36-71 is compared to that of R19.9, and features of the structure responsible for expression of idiotopes are defined.

Added in Proof

Since this paper was accepted for publication, a more highly refined coordinate set has been generated for Fab 36-71. This structure has an *R* factor of 20.9% for all data from 8.0- to 1.9-Å resolution, and an rms deviation of 0.019 Å on bond lengths and 3.99° on bond angles. Although some residues have been repositioned in this structure, the conclusions of this paper are not affected. The Protein Data Bank entry 6FAB contains this structure.

ACKNOWLEDGMENTS

We thank Rebecca To (NRCC) for growing the crystals used for data collection, Dr. Tom Smith (Purdue) for supplying his programs MacFrodo and MacPrep with which many of the figures were prepared, Drs. Greg Farber (Pennsylvania State University) and Barry Stoddard (University of California, Berkeley) for their support and advice, Sanda Teodorescu-Frumosu (Boston University) and Chio-Ying Kao (Boston University) for assistance with some of the experiments involving the characterization of the site-directed mutants, and Payload Systems, (Cambridge, MA) for supplying the DEC Vaxstation 3200.

REFERENCES

Alkan, S. S., Ball, R. K., Chang, J.-Y., & Brown, D. G. (1983) *Mol. Immunol. 20*, 203.

Amzel, L. M., & Poljak, R. J. (1979) *Annu. Rev. Biochem. 48*, 961.

Ball, R. K., Chang, J.-Y., Alkan, S. S., & Braun, D. G. (1983) *Mol. Immunol. 20*, 197.

Brünger, A. T., Kuriyan, J., & Karplus, M. (1987) *Science 235*, 458.

Brünger, A. T., Krukowski, A., & Erickson, J. W. (1990) *Acta Crystallogr. A45*, 585.

Chothia, C., & Lesk, A. M. (1987) *J. Mol. Biol. 196*, 901.

Chothia, C., Lesk, A. M., Tramontano, A., Levitt, M., Smith-gill, S. J., Air, G., Sheriff, S., Padlan, E. A., Davies, D., Tulip, W. R., Colman, P. M., Spinelli, S., Alzari, P. M., & Poljak, R. J. (1989) *Nature 342*, 877–883.

Colman, P. (1988) *Adv. Immunol. 43*, 99.

Cygler, M., Boodhoo, A., Lee, J. S., & Anderson, W. F. (1987) *J. Biol. Chem. 262*, 643.

Davies, D. R., & Metzger, H. A. (1983) *Annu. Rev. Biochem. 1*, 87.

Dodson, G. G. (1981) in *Refinement of protein Structure* (Machin, P. A., Campbell, J. W., & Elder, M., Eds.) p95, Daresbury, London.

Dodson, E. J., Dodson, G. G., Hodgkin, D. C., & Reynolds, C. D. (1979) *Can. J. Biochem. 57*, 469.

Epp, O., Latham, E., Shiffer, M., Huber, R., & Palme, W. (1975) *Biochemistry 14*, 4943.

Estess, P., Lamoyi, E., Nisonoff, A., & Capra, J. D. (1980) *J. Exp. Med. 151*, 863.

Fish, S., & Manser, T. (1987) *J. Exp. Med. 166*, 711.

Fish, S., Zenowich, E., Fleming, M., & Manser, T. (1989) *J. Exp. Med. 170*, 1191.

Fujinaga, M., & Read, R. J. (1987) *J. Appl. Crystallogr. 20*, 517.

Gridley, T., Margolies, M. N., & Gefter, M. L. (1985) *J. Immunol. 134*, 1236.

Haba, S., Rosen, E. M., Meek, K., & Nisonoff, A. (1986) *J. Exp. Med. 164*, 291.

Hartmann, H., Parak, F., Steigemann, W., Petsko, G. A., Ringe, D., & Frauenfelder, H. (1982) *Proc. Natl. Acad. Sci. U.S.A. 79*, 4967.

Hendrickson, W. A. (1979) *Acta Crystallogr. A35*, 158.

Hendrickson, W. A., & Konnert, J. H. (1980) in *Computing in Crystallography* (Diamond, R., Ramaseshan, S., & Venkatesan, K., Eds.) pp 13.01–13.25, Eds.) Indian Academy of Sciences, Bangalore, India.

Howard, A. J., Nielsen, C., Xuong, & Ng, H. (1985) *Methods Enzmol. 114*, 416.

Jerne, N. K. (1974) *Ann. Immunol. (Inst. Pasteur) 125*, 373.

Jeske, D. J., Jarvis, J., Milstein, C., & Capra, J. D. (1984) *J. Immunol. 133*, 1090.

Jones, T. A. (1978) *J. Appl. Crystallogr. 11*, 268.

Kresina, T. F., Rosen, S. M., & Nisonoff, A. (1982) *Mol. Immunol. 19*, 1433.

Kuettner, M. G., Wang, A. L., & Nisonoff, A. (1972) *J. Exp. Med.* 135, 579.

Laemmli, U. K. (1970) *Nature 227*, 680.

Landolfi, N. F., Capra, J. D., & Tucker, P. W. (1986) *J. Immunol. 137*, 362.

Lascombe, M.-B., Alzari, P. M., Boulot, G., Saludjian, P., Tougard, P., Berek, C. Haba, S., Rosen, E. M., Nisonoff, A., & Poljak, R. J. (1989) *Proc. Natl. Acad. Sci. U.S.A. 86*, 607.

Luzzati, V. (1953) *Acta Crystallogr. 6*, 142.

Manser, T., Wysocki, L. J., Gridley, T., Near, R. I., & Gefter, M. L. (1985) *Immuno. Today 6*, 94.

Manser, T., Wysocki, L. J., Margolies, M. N., & Gefter, M. L. (1987a) *Immunol. Rev. 96*, 141.

Manser, T. Parhami-Seren, B., Margolies, M. N., & Gefter, M. L. (1987b) *J. Exp. Med. 166*, 1456.

Margolies, M. N., Marshak-Rothstein, M., & Gefter, M. L. (1981) *Mol. Immunol. 18*, 1065.

Marshak-Rothstein, M., Siekevitz, M., Margolies, M. N., Mudgett-Hunter, M., & Gefter, M. L. (1980) *Proc. Natl. Acad. Sci. U.S.A. 77*, 1120.

Marshak-Rothstein, A., Margolies, M. N., Bendetto, J. D., & Gefter, M. L. (1981) *Eur. J. Immunol. 11*, 565.

Meek, K., Sanz, I., Rathbun, G., Nisonoff, A., & Capra, J. D. (1987) *Proc. Natl. Acad. Sci. U.S.A. 84*, 6344.

Mulligan, R. C., & Berg, P. (1980) *Science 209*, 1422.

Norrander, J., Kempe, J., & Messing, J. (1983) *Gene 26*, 101.

Padlan, E. A., Silverton, E. W., Sheriff, S., Cohen, G. H., Smith-Gill, S. J., & Davies, D. R. (1989) *Proc. Natl. Acad. Sci. U.S.A. 86*, 5938.

Parhami-Seren, B., Wysocki, L., & Margolies, M. N. (1989) *J. Immunol. 143*, 4090.

Parhami-Seren, B., Sharon, J., & Margolies, M. N. (1990) *J. Immunol. 144*, 4426.

Poljak, R. J., Amzel, L. M., Chen, B. L., Phizackerly, R. P., & Saul, F. (1974) *Proc. Natl. Acad. Sci. U.S.A. 71*, 3440.

Ramachandran, G. N., Ramakrishnan, C., & Sasisekharan, V. (1963) *J. Mol. Biol. 7*, 95.

Rathbun, G., Sanz, I., Meek, K., Tucker, P., & Capra, J. D. (1988) *Adv. Immunol. 42*, 95.

Ringe, D., & Petsko, G. A. (1985) *Prog. Biophys. Mol. Biol. 45*, 197.

Rose, D. R., Strong, R. K., Margolies, M. N., Gefter, M. L., & Petsko, G. A. (1990) *Proc. Natl. Acad. Sci. U.S.A. 87*, 338.

Rothstein, T. L., & Gefter, M. L. (1983) *Mol. Immunol. 20*, 161.

Sambrook, J., Fritsch, E. F., & Maniatis, T. (1989) in *Molecular Cloning: A Laboratory Manual*, Cold Spring Harbor Laboratory, Cold Spring Harbor, NY.

Sanger, F., Coulson, A. R., Barrel, B. G., Smith, A. G. H., & Rol, B. A. (1980) *J. Mol. Biol. 143*, 161.

Sanz, I., & Capra, J. D. (1987) *Proc. Natl. Acad. Sci. U.S.A. 84*, 1085.

Segal, D., Padlan, E., Cohen, G. H., Rudikoff, S., Potter, M., & Davies, D. R. (1974) *Proc. Natl. Acad. Sci. U.S.A. 71*, 4298.

Sharon, J. (1990) *Proc. Natl. Acad. Sci. U.S.A. 87*, 4814.

Sharon, J., Gefter, M. L., Manser, T., Morrison, S. L., Oi, V. T., & Ptashne, M. (1984) *Nature (London) 309*, 364.

Sharon, J., Gefter, M. L., Manser, T., & Ptashne, M. (1986) *Proc. Natl. Acad. Sci. U.S.A. 83*. 2628.

Sharon, J., Gefter, M. L., Wysocki, L. J., & Margolies, M. N. (1989) *J. Immunol. 154*, 596.
Sheriff, S., Silverton, E. W., Padlan, E. A., Cohen, G. H., Finzel, B. C., & Davies, D. R. (1987) *Proc. Natl. Acad. Sci. U.S.A. 84*, 8075.
Shimada, A. (1960) *Bull. Chem. Soc. Jpn. 33*, 301.
Shulman, M., Wilde, L., & Kohler, G. (1978) *Nature 276*, 269.
Siegelman, M., & Capra, J. D. (1981) *Proc. Natl. Acad. Sci. U.S.A. 78*, 7679.
Siekevitz, M., Gefter, M. L., Brodeur, P., Riblet, R., & Marshak-Rothstein, A. (1982) *Eur. J. Immunol. 12*, 1023.
Siekevitz, M., Huang, S. Y., & Gefter, M. L. (1983) *Eur. J. Immunol. 13*, 123.
Slaughter, C. A., & Capra, J. D. (1983) *J. Exp. Med. 151*, 863.
Slaughter, C. A., Jeske, D. J., Kuziel, W. A., Milner, E. C., & Capra, J. D. (1984) *J. Immunol. 132*, 3164.
Southern, P. J., & Berg, P. (1982) *J. Mol. Biol. Appl. Genet. 1*, 327.
Strong, R. K., Petsko, G. A., Sharon, J., & Margolies, M. N. (1991) *Biochemistry* (following paper in this issue).
Suh, S. W., Bhat, T. N., Navia, M. A., Cohen, G. H., Rao, D. N., Rudikoff, S., & Davies, D. R. (1986) *Proteins: Struct., Funct., Genet. 1*, 74.
Towbin, H., Staehelin, T., & Gordon, J. (1979) *Proc. Natl. Acad. Sci. U.S.A. 76*, 4350.
Wysocki, L. J., Margolies, M. N., Huang, B., Nemazee, D. A., Wechsler, D. S., Sato, V. L., Smith, J. A., & Gefter, M. L. (1985) *J. Immunol. 134*, 2740.
Wysocki, L. J., Manser. T., & Gefter, M. L. (1986) *Proc. Natl. Acad. Sci. U.S.A. 83*, 1847.
Wysocki, L. J., Gridley, T., Huang, S., Grandea, A. G., III, & Gefter, M. L. (1987) *J. Exp. Med. 166*, 1.
Wysocki, L. J., Gefter, M. L., & Margolies, M. N. (1990) *J. Exp. Med. 172*, 315.
Xuong, Ng, H., Sullivan, D., Nielsen, C., & Hamlin, R. (1985) *Acta Crystallogr. B41*, 267.
Zoller, M. J., & Smith, M. (1983) *Methods Enzymol. 100*, 468.